Mathematical model and dynamic simulink simulation of PEM electrolyzer system

Danxiong Fei[a], Wenwen Fan[b], Zhenlan Dou[c*], Chunyan Zhang[d]

State Grid Shanghai Municipal Electric Power Company of Fengxian, Shanghai, China

Abstract. Hydrogen, being the most abundant element in the universe, holds great promise as an energy carrier for decarbonizing various economic sectors. In particular, green hydrogen production through water electrolysis is essential for achieving this goal, with polymer electrolyte membrane (PEM) water electrolyzers playing a crucial role. PEM water electrolyzers are known for their rapid response, enabling them to effectively adapt to fluctuations in renewable energy sources. Nevertheless, rapid load changes can result in the rapid build-up of heat within the electrolytic cell, leading to a sharp increase in temperature and potentially harming the cell. To address this challenge, we developed an electrolysis water system model using MATLAB and validated its accuracy through experiments. This model allowed us to explore the factors influencing stack temperature and propose a fast and secure dynamic process control strategy. By laying the groundwork for subsequent control studies on PEMEC (Proton Exchange Membrane Electrolysis Cell) stacks and systems, this research facilitates further progress in their control and regulation.

1. Introduction

In the 21st century, humanity faces one of its most significant challenges: mitigating greenhouse gas emissions to curb climate change while meeting the rising energy demands to support economic growth. Renewable energy technology emerges as a crucial solution to address global environmental pollution issues and tackle the energy shortag[1]. Energy sources such as tidal energy, solar energy, and wind energy are location-dependent, intermittent, and hence, less reliable[2]. Hence, efficient energy storage plays a vital role in enabling widespread and dependable utilization of renewable energy technology. Hydrogen serves as an environmentally friendly fuel option[3]. Utilizing surplus renewable power to operate water electrolyzers for water-splitting represents a promising approach for storing excess renewable energy[4].

In recent years, much of the research has been centered around proton exchange membrane (PEM) electrolysis technology due to its numerous advantages over alkaline electrolyzer cells. These advantages include higher current density, enhanced hydrogen purity, non-hazardous liquid electrolyte, and most notably, a rapid transient response, making it highly suitable for applications in renewable energy systems.[5].

There are numerous experimental studies investigating the PEM electrolyzers in different aspects[6]. Indeed, models play a vital role in electrolyzer development as they provide valuable insights into the impact of various parameters on electrolyzer performance, enabling efficient simulation, design, and optimization of electrolyzer systems. Moreover, experimental data collection can be challenging, especially in complex systems or specific conditions. To tackle the dynamic challenges of connecting an intermittent electrical source to an electrolysis system, modeling emerges as a critical and powerful tool for understanding phenomena, conducting control analysis, sizing components, managing energy, and optimizing system performance.[7].

Concerning the state-of-the-art PEM electrolyzer modeling, while there are well-established simulations available in the literature, there remains a limited number of dynamic modeling studies specifically related to PEM electrolysis. Á. Hernández-Gómez[8] constructed an equivalent circuit model for the electrolytic cell and studied its dynamic response process. They accurately simulated the voltage dynamic behavior of the electrolytic cell. Math model also was developed by many works[9]. Models have been perfect simulated the effects of pressure, temperature and current density in stack[10]. Transient operations pose higher demands on system control, and models serve as effective tools for studying dynamic system operations. Therefore, dynamic PEM water electrolysis has sparked considerable interest among researchers. Haluk Görgün explored a model to predict the stack voltage, gas tank pressure and stack efficiency under dynamic operation[7b]. Furthermore, the literature also presents more complex models that consider mass transfer and multi-physics field coupling[11].

[a]feidanxiong@sh.sgcc.com.cn, [b]fanwenwen@sh.sgcc.com.cn, [c*]douzhl@126.com, [d]zhcytongji@126.com

Although many researchers have made extensive efforts in modeling PEM water electrolysis, there has been limited research on the extreme conditions experienced by the electrolytic cell under fluctuating inputs. Investigating extreme conditions is crucial for ensuring the safe operation of the electrolytic cell. To assess the performance of a PEM electrolyzer system, gain insights into the dynamic response characteristics of the system and its individual components, and design superior systems for the future, we developed a dynamic model of a PEM electrolyzer system using MATLAB. This model was utilized to study the system's response patterns under extreme fluctuating conditions. Additionally, the paper proposes corresponding control strategies to effectively address these challenging scenarios.

2. Model description

2.1. Voltage

The electrolyzer voltage (V) using the following expression:

$$V = N_C(E_{Cell} + V_{ACt} + V_{Diff} + V_{Ohm}) \quad (1)$$

where Nc is the number of electrolyzer cells, E_{Cell} is the open circuit voltage V_{ACt} are the anode activation overpotentials and cathode was neglect, V_{Ohm} is the electrolyzer cell resistance (ohmic losses). Similar expressions are used by almost all the authors[12].

The open circuit voltage is typically determined using the Nernst equation, which is a widely used equation found in numerous works reported in the literature, or variations of it are utilized for the same purpose.

$$E_{cell} = E^0_{rev} + \frac{RT}{2F}[\ln(\frac{{P_{H_2}P_{H_2}}^{1/2}}{P_{H_2O}})] \quad (2)$$

where P is the partial pressure of reactants/products, T is the temperature, F is the Faraday constant and E^0_{rev} is the reversible cell potential at standard temperature and pressure. It is calculated by

$$E^0_{rev} = 1.229 - 0.9 \times 10^{-3}(T - 298) \quad (3)$$

Activation losses occur, as mentioned, due to the need to allocate some potential for activating the electrochemical reactions occurring at the anode and cathode sides. One of the more commonly used expressions for calculating activation overpotential is based on the Butler-Volmer equation.

$$V_{Act} = \frac{RT_a}{\alpha_a F}\arcsin(\frac{i}{2i_{0,a}}) + \frac{RT_c}{\alpha_c F}\operatorname{arcsinh}(\frac{i}{2i_{0.c}}) \quad (4)$$

where $i_{0,a}$ and $i_{0,c}$ are the exchange current density at anode and cathode, respectively and α_a and α_c are the charge transfer coefficients at anode and cathode, respectively. i_0 increase with temperature, Therefore, to relate it with the temperature, an expression is presented by applying an Arrhenius expression, as follows:

$$i_0 = i_{0,ref}exp[-\frac{E_{act}}{R}(\frac{1}{T} - \frac{1}{T_{ref}})] \quad (5)$$

where $E_{act}$is the activation energy of the electrode and $i_{0,ref}$ is the exchange current density measured at a reference temperature T_{ref}.

M. Lebbal used an expression based on i_{lim} , The maximum current density that the electrolyzer can handle determines the maximum production rate allowed by the electrolyzer. [13]:

$$V_{Diff} = -\frac{RT}{nF}\ln(1 - \frac{i}{i_{lim}}) \quad (6)$$

The ohmic overpotential is associated with the material's resistance to the flow of protons. The standard Ohm's law is applied in the analysis of the work.

$$V_{Ohm} = RI = \frac{\delta}{\sigma}I \quad (7)$$

where δ is the material thickness and σ the material conductivity. The membrane conductivity, considering Nafion, can be expressed as

$$\sigma = \left(0.005139\lambda - 0.00326\right)\exp\left[1268\left(\frac{1}{303} - \frac{1}{T}\right)\right] \quad (8)$$

where T is the electrolyzer temperature and λ is the membrane water content[14].

2.2. Lumped parameters thermal models

Temperature positively influences the reversible potential value. Additionally, since activation, ionic diffusion, electronic diffusion, and matter transfer are thermally activated processes, temperature also has a beneficial impact on the overall cell voltage. In this study, the stack is treated as a single thermal capacitance (lumped thermal capacitance), and its temperature is assumed to be uniform.

Considering the various input-output enthalpy flows on the electrolysis stack and assuming no water evaporation, the stack's enthalpy balance can be expressed as follows: [Please provide the specific equation for the enthalpy balance if available, as it was cut off in the given text[14]:

$$C_{th}\frac{dT}{dt} = \sum h_i^{in}N_i^{in} - \sum h_i^{p}i_i^{put} + Q_{net} \quad (9)$$

where h_i is the specific enthalpy of species i, and N_i is the molar flow rate of the corresponding species in or out of the electrolyzer. The lumped thermal capacitance or overall thermal capacity, C_{th} , is the sum of the component thermal capacities

$$C_{th} = \sum \rho_j V_j C_{p,j} \quad (10)$$

in which ρ_j , V_j , and $C_{p,j}$ are the values for density, volume, and heat capacity of each component, respectively. The net heat generation, Q_{net} , is composed of varied heat sources and sinks in the system.

$$Q_{net} = Q_{gen} - Q_{loss} - Q_{cost} - Q_{misc} \quad (11)$$

the terms described in the net heat generation of the system include Q_{gen} , Q_{loss} , Q_{cost} , Q_{misc} which describe

heat generation, loss, cooling, and other miscellaneous phenomena, respectively.

3. Results and discussion

We initially conducted experiments using a 10 kW system to validate the reliability of the model. The verification was done by comparing the I-V (current-voltage) curves obtained from the experiments with the model predictions(Figure 1). This method is commonly used to assess the reliability of PEM water electrolysis models. In the 10 kW system, experiments were carried out at 50°C, and from the comparison shown in the graph, it can be concluded that the model exhibits good accuracy and provides reliable predictions.

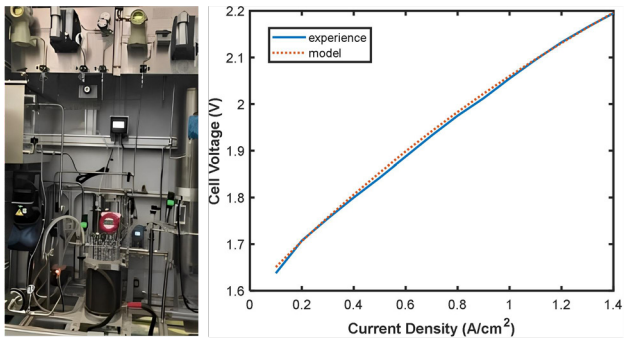

Figure 1. Model validation by 10kw test bench

Figure 2 illustrates the impact of current step changes on the electrolytic cell temperature and the electrolytic cell outlet temperature. From the graph, it can be observed that when the current density jumps from 0A/cm^2 to 1 A/cm^2, the electrolytic cell temperature rapidly increases within 5 seconds, rising from around 323K to 329K, and finally stabilizes. In contrast, the electrolytic cell outlet water temperature shows only a slight increase of approximately 1K. This is because when the current increases, the heat generation in the cell stack also increases. Unlike fuel cells that have dedicated cooling fluids, water serves as both a reactant and a coolant for the electrolytic cell. Due to slow heat transfer and the presence of thermal resistance, the heat generated in the electrolytic cell cannot be fully dissipated, leading to its accumulation inside the cell, especially on the Membrane Electrode Assembly (MEA). This heat accumulation causes the rapid rise in the electrolytic cell temperature. Therefore, when the current input suddenly increases, the outlet water temperature of the electrolytic cell rises slowly and with a smaller magnitude, while the electrolytic cell temperature rapidly increases.

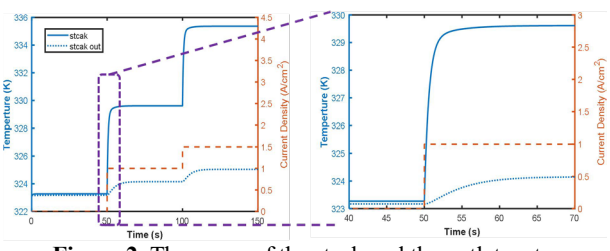

Figure 2. The curve of the stack and the outlet water temperature of the stack varying with the current step change.

Figure 3 illustrates the influence of current step changes on the voltage. The graph shows a voltage difference of 10-20mV between the periods before and after the 1 A/cm^2 step change. It can be observed that when the current undergoes a step change, the voltage instantaneously increases, followed by a slow decrease within a few seconds until it reaches a stable level. This phenomenon occurs because the electrolysis voltage responds instantaneously to the abrupt change in input current. Subsequently, within a few seconds, the electrolytic cell temperature rapidly increases, which leads to a reduction in voltage. Eventually, when the temperature stabilizes, the voltage also stabilizes, and further changes are no longer observed.

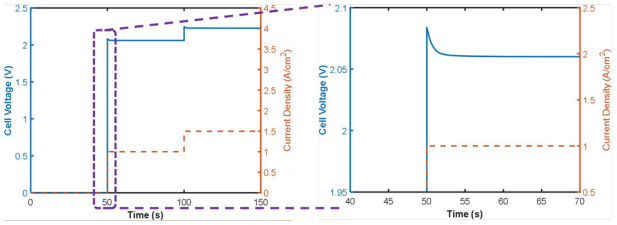

Figure 3. The impact of current step changes on the electrolytic cell voltage.

The electrolytic cell temperature significantly affects the performance and lifespan of the cell. Therefore, studying the temperature variation during fluctuations is of crucial importance. Figure 4 illustrates the trend of electrolytic cell temperature under different current step changes. It can be observed that while the step change in current density exceeds 3.5A/cm^2, the electrolytic cell temperature will rapidly increases and exceed 373K, which greatly exceeds the allowable usage temperature of the Nafion membrane. While temperature spikes are also influenced by factors such as water inflow rate and the material of the electrolytic cell, this indicates that the adaptability of the electrolytic cell to fluctuations has its limits.

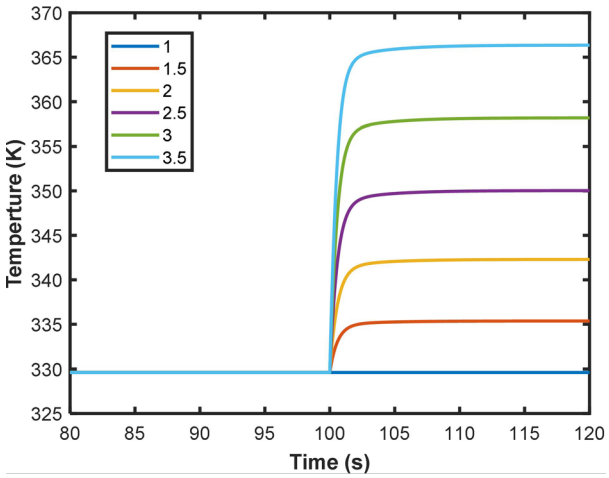

Figure 4. The effect of different step changes in current density(A/cm^2) on the electrolytic cell temperature.

Figure 5 illustrates the impact of different water inflow rates (5 kg/s, 7 kg/s, 9 kg/s) on the electrolytic cell temperature during current step changes. It can be

observed that increasing the water inflow rate helps to lower the electrolytic cell temperature. However, when the water inflow rate becomes excessively high, the cooling effect of further increasing the water inflow rate becomes very limited. For instance, when the water inflow rate nearly doubles (from 5 kg/s to 9 kg/s), the change in the electrolytic cell temperature is only 2K.

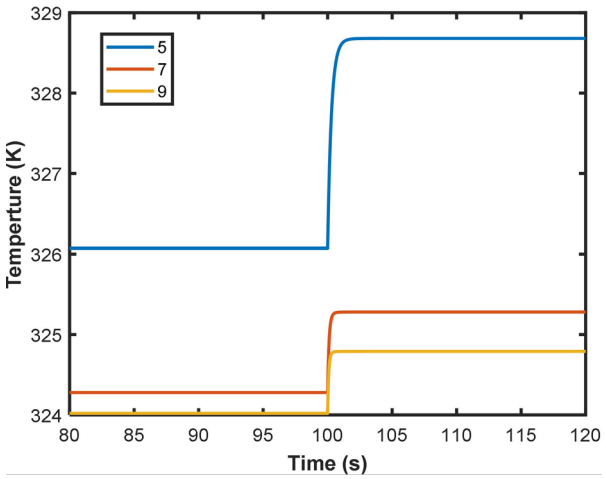

Figure 5. The effect of water inflow rate on the stack temperature(The current jumps from 0A/cm^2 to 1A/cm^2.).

Figure 6 illustrates the impact of different water inflow temperatures (293.15K, 303.15K, 313.15K, 323.15K) on the electrolytic cell temperature during current step changes. It can be observed that lowering the water inflow temperature effectively reduces the electrolytic cell temperature. Compared to adjusting the water flow rate into the electrolytic cell, reducing the water inflow temperature is more effective in mitigating the risk of excessive temperature rise in the electrolytic cell, especially when dealing with larger current fluctuations.

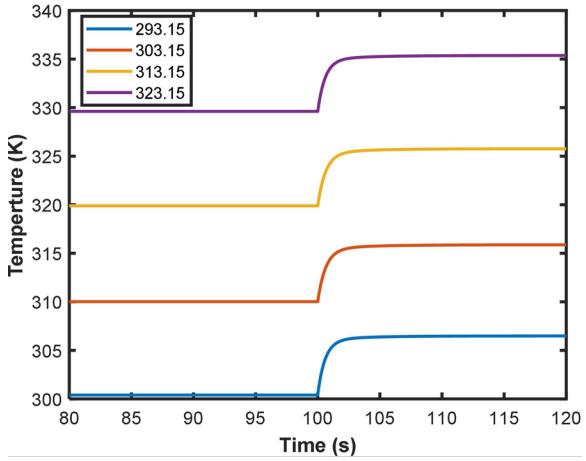

Figure 6. The effect of water inflow temperture on the stack temperature(The current jumps from 0A/cm^2 to 1A/cm^2.).

4. Conclusions

This study developed a system-level simulation model to assess the impact of current input fluctuations on the temperature of PEM water electrolytic cells. The results indicate that fluctuating input currents have a significant effect on the electrolytic cell temperature, especially when the current suddenly increases, leading to a rapid temperature rise in the electrolytic cell. Excessive current fluctuations can cause the electrolytic cell temperature to exceed the allowable temperature of the Nafion membrane, resulting in cell failure and potential safety issues.

To mitigate the rapid temperature rise caused by current step changes, increasing the water inflow can be effective, but it might be costly and less effective for small current step changes. However, for larger current step changes, the effect becomes more pronounced. Therefore, to prevent the electrolytic cell temperature from soaring and damaging the cell due to fluctuating inputs, two approaches can be considered. On one hand, setting an upper limit for the electrolytic cell input can be implemented, and on the other hand, increasing the water inflow appropriately during periods of significant current fluctuations may be necessary.

References

1. C. Intergovernmental Panel on Climate, Climate Change 2013 – The Physical Science Basis: Working Group I Contribution to the Fifth Assessment Report of the Intergovernmental Panel on Climate Change, Cambridge University Press, Cambridge, 2014.
2. aR. Clarke, S. Giddey, F. Ciacchi, S. Badwal, B. Paul, J. Andrews, International journal of hydrogen energy 2009, 34, 2531-2542; bF. Grueger, O. Hoch, J. Hartmann, M. Robinius, D. Stolten, International Journal of Hydrogen Energy 2019, 44, 4387-4397.
3. aS. Griffiths, B. K. Sovacool, J. Kim, M. Bazilian, J. M. Uratani, Energy Research & Social Science 2021, 80, 102208; bA. M. Oliveira, R. R. Beswick, Y. Yan, Current Opinion in Chemical Engineering 2021, 33, 100701.
4. aA. Boretti, B. K. Banik, Advanced Energy and Sustainability Research 2021, 2, 2100097; bM. Oertel, J. Schmitz, W. Weirich, D. Jendryssek-Neumann, R. Schulten, Chemical Engineering & Technology 1987, 10, 248-255.
5. aR. E. Clarke, S. Giddey, F. T. Ciacchi, S. P. S. Badwal, B. Paul, J. Andrews, International Journal of Hydrogen Energy 2009, 34, 2531-2542; bB. Laoun, A. Khellaf, M. W. Naceur, A. M. Kannan, International Journal of Hydrogen Energy 2016, 41, 10120-10135; cA. Mraoui, B. Benyoucef, L. Hassaine, International Journal of Hydrogen Energy 2018, 43, 3441-3450.
6. aP. Millet, in Electrochemical Technologies for Energy Storage and Conversion, 2011, pp. 383-423; bP. Millet, S. Grigoriev, in Renewable Hydrogen Technologies (Eds.: L. M. Gandía, G. Arzamendi, P. M. Diéguez), Elsevier, Amsterdam, 2013, pp. 19-41; cK. Zeng, D. Zhang, Progress in Energy and Combustion Science 2010, 36, 307-326.
7. aZ. Abdin, C. J. Webb, E. M. Gray, International Journal of Hydrogen Energy 2015, 40, 13243-

13257; bA. Awasthi, K. Scott, S. Basu, International Journal of Hydrogen Energy 2011, 36, 14779-14786; cF. d. C. Lopes, E. H. Watanabe, in 2009 Brazilian Power Electronics Conference, 2009, pp. 775-782.
8. aÁ. Hernández-Gómez, V. Ramirez, D. Guilbert, B. Saldivar, Renewable Energy 2021, 163, 1508-1522; bÁ. Hernández-Gómez, V. Ramirez, D. Guilbert, International Journal of Hydrogen Energy 2020, 45, 14625-14639.
9. aP. Colbertaldo, S. L. Gómez Aláez, S. Campanari, Energy Procedia 2017, 142, 1468-1473; bB. Han, S. M. Steen, J. Mo, F.-Y. Zhang, International Journal of Hydrogen Energy 2015, 40, 7006-7016.
10. T. M. Brown, J. Brouwer, G. S. Samuelsen, F. H. Holcomb, J. King, Journal of Power Sources 2008, 182, 240-253.
11. aM. Maier, K. Smith, J. Dodwell, G. Hinds, P. Shearing, D. Brett, International Journal of Hydrogen Energy 2022, 47, 30-56; bP. Olivier, C. Bourasseau, P. B. Bouamama, Renewable and Sustainable Energy Reviews 2017, 78, 280-300.
12. aZ. Abdin, C. Webb, E. M. Gray, International journal of hydrogen energy 2015, 40, 13243-13257; bA. M. Abomazid, N. A. El-Taweel, H. E. Farag, IEEE Transactions on Industrial Informatics 2021, 18, 5870-5881; cE. Afshari, S. Khodabakhsh, N. Jahantigh, S. Toghyani, International Journal of Hydrogen Energy 2021, 46, 11029-11040.
13. M. Lebbal, S. Lecœuche, International journal of hydrogen energy 2009, 34, 5992-5999.
14. G. S. Ogumerem, E. N. Pistikopoulos, Smart and Sustainable Manufacturing Systems 2018, 2, 25-43.